energies

MDPI

Article

Influence of Oxymethylene Ethers (OME_n) in Mixtures with a Diesel Surrogate †

Sandra Richter *, Trupti Kathrotia, Marina Braun-Unkhoff, Clemens Naumann and Markus Köhler

German Aerospace Center (DLR), Institute of Combustion Technology, Pfaffenwaldring 38-40, 70569 Stuttgart, Germany; trupti.kathrotia@dlr.de (T.K.); Marina.Braun-Unkhoff@dlr.de (M.B.-U.); Clemens.Naumann@dlr.de (C.N.); m.koehler@dlr.de (M.K.)

* Correspondence: Sandra.Richter@dlr.de

† This paper is an extended version of our paper published in the 10th European Combustion Meeting (ECM), virtual conference, 14–15 April 2021.

Abstract: Within this work the effects of blending oxymethylene ethers (OME_n) to a diesel surrogate (50 mol% n-dodecane, 30 mol% farnesane, and 20 mol% 1-methylnaphthalene) were investigated by performing two different types of experiments: measurements of the sooting propensity and of the laminar burning velocity, each in laminar premixed flames. For the sooting propensity, OME_3, OME_4, and OME_5 were considered as blending compounds—each in mass fractions of 10%, 20%, and 30%. The sooting propensity was found to depend strongly on the OME_n blending grade but not on its chain length. In addition, the effect on the laminar burning velocity was studied for OME_4 and the admixture of 30% OME_4 with diesel surrogate for the first time. This admixture was found to lead to increased burning velocities; however, much less than might be foreseen when considering the respective values of the neat fuels.

Keywords: oxymethylene ether; alternative fuel; diesel; laminar burning velocity; sooting propensity; road transport

Citation: Richter, S.; Kathrotia, T.; Braun-Unkhoff, M.; Naumann, C.; Köhler, M. Influence of Oxymethylene Ethers (OME_n) in Mixtures with a Diesel Surrogate. *Energies* **2021**, *14*, 7848. https://doi.org/10.3390/en14237848

Academic Editors: Goutham Kukkadapu and Evangelos G. Giakoumis

Received: 29 September 2021
Accepted: 19 November 2021
Published: 23 November 2021

1. Introduction

In recent years, different kinds of synthetic fuels became points of interest as alternative fuel compounds for diesel engines; besides the long known biodiesel (FAME/fatty acid methyl ester), oxymethylene ethers (OME_n: $H_3CO(H_2CO)_nCH_3$) and also alcohols (see e.g., [1]) are under consideration. Particularly, OME_n attracted much interest for application in diesel engines due to several reasons [2]. (I) The absence of C-C bonds (see Figure 1) results in highly reduced formation of soot precursors and soot, even for fuel-rich mixtures, when compared to conventional or other oxygenated fuels, such as alcohols, as well as to biodiesel. Hence, the use of OME_n as a drop-in fuel not only promises a substantially stronger reduction of soot emission but, even more so, an escape from the trade-off between soot and nitrogen oxides (NO_x). (II) OME_n can be produced from renewable sources—either via the power-to-liquid (PtL) process or from sustainable resources (biomass) via gasification or fermentation. (III) Although OME_n do not have any C-C bonds, they are fully miscible with conventional hydrocarbon fuels and, in particular, higher OME_n ($n \geq 2$) are in accordance with important fuel properties; e.g., the boiling temperatures of OME_{2-5} range from 105 °C to 280 °C [3] compared to the boiling range of 85 °C to 360 °C for conventional diesel fuels [4]. With cetane numbers (CN) of 63 for OME_2 up to 100 for OME_5 [3], the admixture of OME_{2-5} can improve the ignition behavior of a diesel fuel, where a minimum CN of 51 is required, according to the standard EN 590 [4]. For these reasons it is expected that blends of OME_n with diesel can be used in engines with modified sealing material [5,6]. Omari et al. [5] have replaced NBR (acrylonitrile butadi-

ene rubber) and FKM (fluorinated rubber) sealings by PTFE (polytetrafluorethylene) sealings for their engine tests and emission measurements with different diesel and OME_n blends. Similarly, Pélerin et al. [6] have tested different materials for their engine tests. Besides PTFE, they have identified FFKM (perfluorelastomer) as a suitable material for a combined application of OME_n and diesel fuel. Other modifications, e.g., on the fuel injector, were reported to be unnecessary.

Regarding experimental studies focusing on the combustion properties of higher OME_n ($n \geq 2$), only a limited database is available in literature. Particularly, data for their laminar burning velocities are rare—in 2017 Sun et al. [7] published measurements of OME_3 at 1 atm and 408 K; recently, those of OME_2 were studied by Eckart et al. [8] and Ngugi et al. [9] at various temperatures and pressures. Though engine tests are often performed, e.g., such as those reported in Omari et al. [5] and Pélerin et al. [6], basic studies focusing on the sooting behavior are rare. Here, the influence of OME_n on the sooting behavior of a diesel fuel was studied recently by Palazzo et al. [10] for the addition of OME_2 and OME_{3-5} in a laminar diffusion flame.

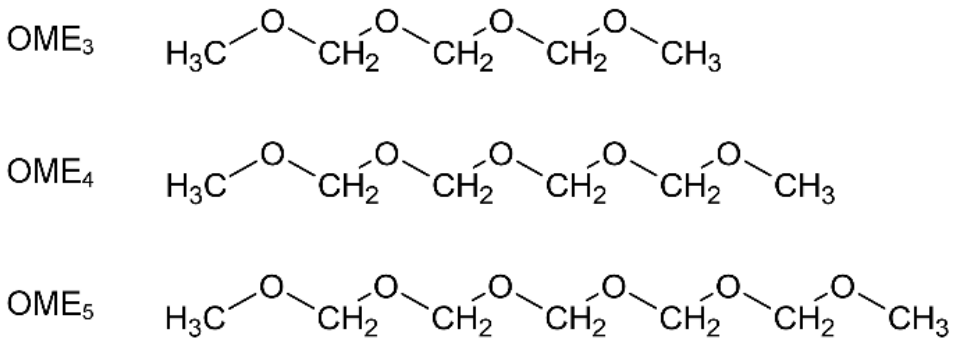

Figure 1. Molecular structures of OME_3, OME_4, and OME_5.

In order to improve the understanding on the influence of OME_n when blended in a diesel fuel, the aim of the present work is to investigate the combustion characteristics by performing two kinds of experiments: measurements of (I) the sooting propensity and of (II) the laminar burning velocity (LBV). Each experiment was conducted by the use of a laminar premixed flame. For the determination of the sooting propensity, OME_3, OME_4, and OME_5 were added in different concentrations to a well-known diesel surrogate consisting of 50% n-dodecane, 30% farnesane (2,6,10-trimethyldodecane), and 20% 1-methylnaphthalene (all mole percentages), which are capable of representing relevant diesel fuel properties. Regarding LBV, OME_4 is in the focus of this work, being measured as neat fuel as well as in a mixture with the diesel surrogate. To the best of our knowledge, experimental LBV data of neat OME_4 as well as of a hydrocarbon and OME_4 mixture are presented for the first time. For comparison, LBV values of the neat diesel surrogate was measured as well. The experimentally determined values of the burning velocities were compared to and analyzed with calculated laminar flame speeds using a recently developed reaction mechanism [11] to investigate the observed effects in more detail [12].

2. Materials and Methods

For both type of experiments, a surrogate for a fossil-based diesel fuel was prepared consisting of 50% n-dodecane, 30% farnesane (2,6,10-trimethyldodecane), and 20% 1-methylnaphthalene (mole percentages). Using this composition, the diesel surrogate mirrors the chemical composition—with each a representative for n-alkanes, iso-alkanes, and aromatics—as well as major relevant physical properties of a diesel fuel, such as the boiling temperature, in a range from 215 °C to 250 °C. The specific purities and supplier of the used surrogate components as well as of the considered OME_n are listed in Table 1.

The sooting propensity of the diesel surrogate and the influence of OME_n were studied using OME_3, OME_4, and OME_5 as mixing components; in total, nine different mixtures

of diesel surrogate and OME_n were studied. The focus was set (I) to investigate, if existing, the possible dependence on the length of the OME_n, and (II) to examine the effect of the OME_n-addition to the diesel surrogate. For the latter, the OME_n concentrations in each blend of diesel surrogate and OME_n considered were 10% *(w/w)*, 20% *(w/w)*, and 30% *(w/w)*. An overview about the measured blends is given in Table 2.

For the investigation of the effect of the addition of OME_n on the laminar burning velocity of the surrogate-OME mixture, the fuels measured were: (I) the diesel surrogate, (II) pure OME_4, and (III) diesel surrogate and 30% *(w/w)* OME_4. The measurements were conducted with 473 °K as preheat temperature and at ambient as well as elevated pressures (1 bar, 3 bar, and 6 bar) over a wide range of the fuel–air equivalence ratio (φ), listed in detail in Table 2.

Table 1. Overview of the specific purity and supplier of the surrogate components and considered oxymethylene ether (OME_n).

Component/OME_n	Purity	Supplier
n-Dodecane	≥99%	Sigma–Aldrich
Farnesane	≥98%	Sigma–Aldrich
1-Methylnaphthalene	≥94%	Merck
OME_3	98.67%	ASG
OME_4	98.25%	ASG
OME_5	97.20%	ASG

Table 2. Overview about the considered fuel mixtures and performed experiments at a preheat temperature each of T = 473 K.

Fuels/Fuel Mixtures	Sooting Propensity	Laminar Burning Velocity
OME_4		p = 1 bar/p = 3 bar/p = 6 bar φ = 0.8-2.0/φ = 0.7-1.6/φ = 0.8–1.5
Diesel surrogate (=50 mol% n-dodecane +30 mol% farnesane +20 mol% 1-methylnaphthalene)	p = 1 bar	p = 1 bar/p = 3 bar/p = 6 bar φ = 0.6-1.7/φ = 0.7-1.6/φ = 0.7–1.5
+10% *(w/w)* OME_3	p = 1 bar	
+20% *(w/w)* OME_3	p = 1 bar	
+30% *(w/w)* OME_3	p = 1 bar	
+10% *(w/w)* OME_4	p = 1 bar	
+20% *(w/w)* OME_4	p = 1 bar	
+30% *(w/w)* OME_4	p = 1 bar	p = 1 bar/p = 3 bar/p = 6 bar φ = 0.6-1.8/φ = 0.7-1.6/φ = 0.6–1.5
+10% *(w/w)* OME_5	p = 1 bar	
+20% *(w/w)* OME_5	p = 1 bar	
+30% *(w/w)* OME_5	p = 1 bar	

2.1. Determination of the Sooting Propensity

The experimental set-up for the measurement of the sooting propensity is shown in Figure 2 and consists of four parts: (I) The preparation of the fuel–air mixture; (II) the burner; (III) the sampling probe; and (IV) the particle detection unit. The determination of the sooting propensity has already been previously described [13,14], so only a short description is given here.

For the preparation of the fuel–air mixture (I), the liquid fuel is vaporized using a HPLC-pump (LC-20AD, Shimadzu) to feed the vaporizer [15]. First, the vaporized fuel is

mixed with a preheated nitrogen stream (N_2—99.999%, Linde gas) and conditioned to the set temperature of T = 473 K. In a second mixing step, oxygen (O_2—99.95%, Linde gas) is added according to the N_2/O_2-ratio in the air. The gas flows are controlled by mass flow controllers (mini Cori-Flow, Bronkhorst). The burner (II) is constructed as a type of Bunsen burner. Here, a premixed planar flame is ignited at a nozzle heated to 473 K as well. The nozzle is made of copper, has an outlet diameter of 12 mm, and contains a fine-pored sinter plate needed to stabilize the planar flame. The gas velocity of the unburned fuel–air mixture is kept constant at 35 cm/s during all the measurements. To avoid disturbance from the environment, the flame is shielded by a quartz cylinder, and a purified air coflow is streaming in between the nozzle and the quartz cylinder.

The sampling unit (III) consists of three concentric pipes, as shown in Figure 3; it is fixed above the burner and reaches out into the exhaust gas. The outer pipe is made from quartz glass and has a cone with a fine orifice at the tip, where the exhaust gas from the flame is expanded into the inner central pipe made from stainless steel. In the middle pipe (made from Pyrex glass), nitrogen (N_2; 99.999%, Linde) is added to delay particle coagulation in the exhaust gas by dilution. Through the inner pipe the sample is transferred into the particle counter (CPC 3022A, TSI) with a flow rate of 1.5 L/min generated by the particle counter. The nitrogen flow is adjusted to about 1.4 L/min, so that the pressure inside the sampling unit is kept constant at about 0.9 bar. A pressure control valve and two pressure transducers (0–1 bar absolute, Schaevitz) are connected to the sampling unit to make sure that no pressure overload occurs, which could lead to a failure of the measurement and a damage of the particle counter. Particles are detected upon a minimum size of 0.007 µm.

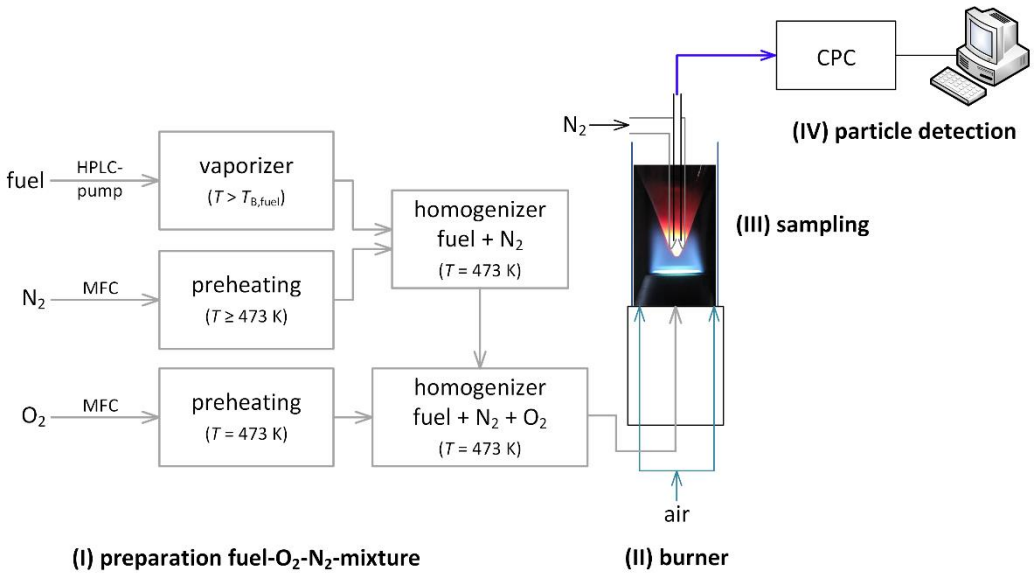

Figure 2. Scheme of the experimental set-up for the measurement of particle concentration in the exhaust gas of a plane-laminar flame. The specific preheating temperature of nitrogen is at least 473 K, subjected to the final boiling of the fuel mixture; CPC—condensation particle counter, HPLC—high performance liquid chromatography, MFC—mass flow controller, $T_{B,fuel}$—final boiling point of the fuel mixture.

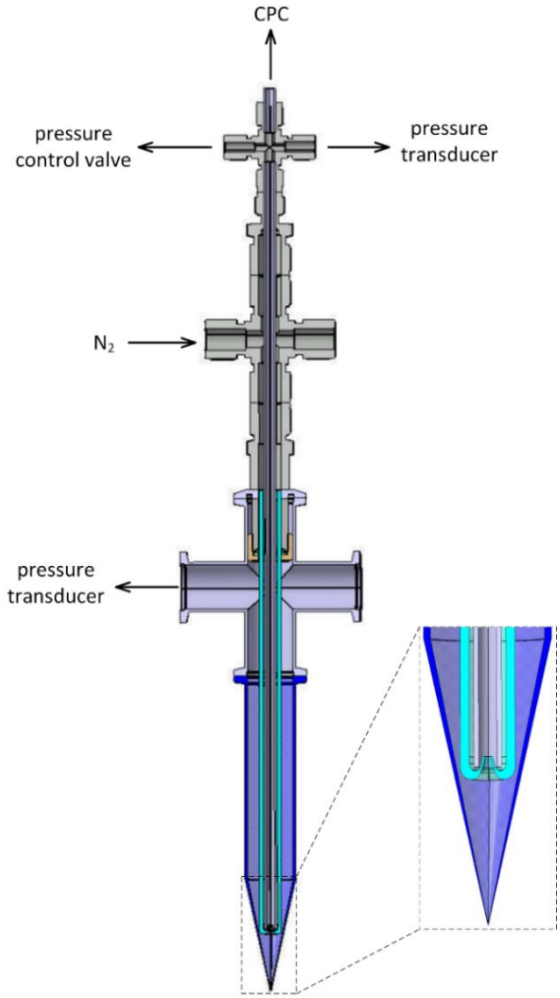

Figure 3. Scheme of the sampling unit used for the measurement of the sooting propensity (inlets, as they were not labeled, were closed during the measurement); CPC—condensation particle counter.

Starting with $\varphi = 1.40$, the fuel fraction is increased during the measurement. As soon as the particle concentration starts to rise, the φ value is kept constant for 15 min. The particle concentration is measured at a sampling rate of 6 min^{-1}, i.e., datapoints were recorded every 10 s.

For the evaluation, the first three minutes are skipped in order to allow the slight time delay between the increase of the fuel volume flow and the adjustment of the φ value after the fuel–air ratio was changed. In addition, all particle concentrations were normalized to 10^4 particles/cm^3; the corresponding φ value was determined by interpolation. As a measure for the sooting propensity, the φ value, defined as the soot threshold value (φ_{ST}), is obtained from the maximum gradient of the normalized particle concentration by extrapolation to the baseline, as shown in Figure 4, for the diesel surrogate and the mixtures with OME_5. In detail, the determination of φ_{ST} is visualized for the mixture diesel surrogate and 30% *(w/w)* OME_5, where the tangent line at the maximum gradient (corresponding to the highest increase of the particle concentration in the exhaust gas) is drawn. The extrapolation of the tangent line to the base line (particle concentration = 0.0) yields a soot threshold value of $\varphi_{ST} = 1.78$. The uncertainty of the calculated soot thresholds is ± 0.005, as determined from the performance of at least three repeated measurements of each diesel surrogate and OME_n mixture.

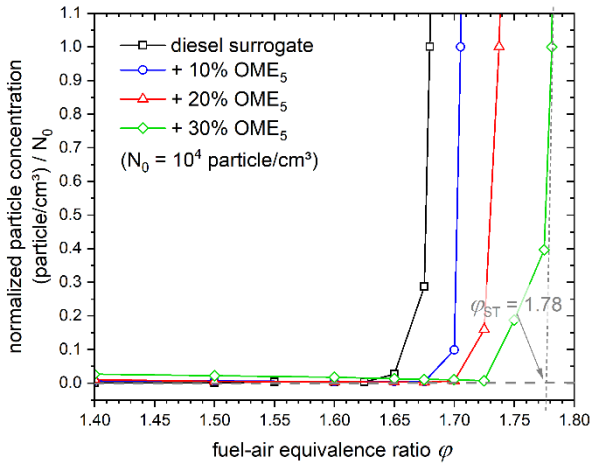

Figure 4. Normalized particle concentrations for the diesel surrogate and the surrogate-OME_5 mixtures (percentage given in mass fraction) showing the extrapolation to the soot threshold (φ_{ST}). The grey dashed tangent line indicates the maximum gradient of the increasing particle concentration for the mixture of the diesel surrogate with 30% *(w/w)* OME_5 and is extrapolated to the base line where the intersection gives the value for φ_{ST}.

2.2. Determination of the Laminar Burning Velocity

The experimental set-up for the measurement of the laminar burning velocity (LBV) is depicted in Figure 5. As visible, the preparation of the fuel–air mixture (I) and the burner (II) are identical to the experimental set-up for the determination of the sooting propensity. However, whereas for the sooting propensity a planar flame with a constant gas flow is used, here, for measuring LBV, a conical flame is stabilized using different nozzles (all without the sinter plate) of outlet diameters between 3 cm and 8 cm. The nozzle to be used depends on the considered conditions: for measurements at 1 bar, nozzles with outlet diameters of 6 cm and 8 cm were used, at 3 bar, a nozzle with 4 cm was used, and at 6 bar, 3 cm was used. In contrast to the measurement of the sooting propensity, these measurements were performed with a housing around the nozzle. This enables measurements at elevated pressures and the use of different coflows. For more detailed information of the technique, see, e.g., [16–18].

By using a coflow, with either air for fuel-rich flames ($\varphi \geq 1.0$) or a mixture of 5% CH_4, 5% H_2, and 90% N_2 (prepared by Linde) for fuel-lean flames ($\varphi \leq 1.0$), premixed flames have been stabilized to measure the LBV. At fuel-rich conditions, the use of air as the coflow leads to the post-combustion of unburned hydrocarbons in the exhaust gas; for fuel-lean flames, the post-combustion of the excess oxygen is enabled, due to the use of the $CH_4/H_2/N_2$ coflow. Without post-combustion, the range of the fuel equivalence ratio for the determination of the laminar burning velocity is (too) limited, due to the occurrence of unstable flames—resulting in the flame liftoff—caused by an increased quenching distance to the nozzle when the φ value is reduced. Tests with other coflow mixtures—including a pure N_2 coflow—show that there is practical no influence on the specific flame angle selected due to the use of this specific coflow. Hence, the $CH_4/H_2/N_2$ coflow at fuel-lean conditions has the same stabilizing effect as the air coflow at fuel-rich conditions. It also influences the quenching distance at the nozzle rather than the heat release at the flame surface, remaining diffusion limited; therefore, it is much more distributed than the flame front representing the conical flame. Buoyancy effects due to density gradients between coflow and exhaust gas, i.e., stretching of the cone, were not important at all due to the small height of the flame.

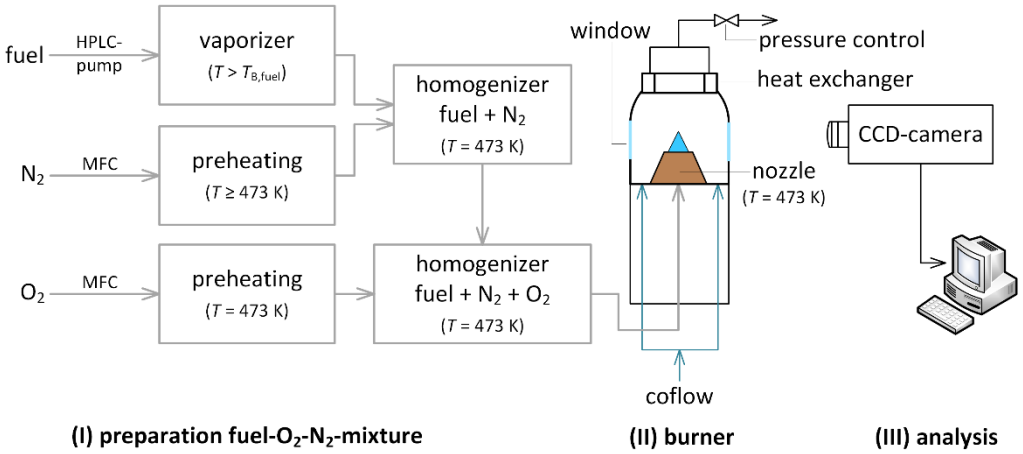

Figure 5. Scheme of the experimental set-up for the measurement of the laminar burning velocity of a conical laminar flame. The temperature of the nitrogen preheating depends on the final boiling of the fuel mixture but is at least 473 K; HPLC—high performance liquid chromatography, MFC—mass flow controller, $T_{B,fuel}$—final boiling point of the fuel mixture.

For the cone angle detection within the analysis section (III) pictures with a CCD-camera (Imager Intense, LaVision) were recorded using an exposure time of 0.2 s. The laminar burning velocity (S_u) is calculated from the measured cone angle (α) of the flame and the gas velocity (v_u) of the unburned fuel–air mixture, as illustrated in Figure 6 according to Equation (1) [19,20]:

$$S_u = v_u \cdot \sin \alpha. \quad (1)$$

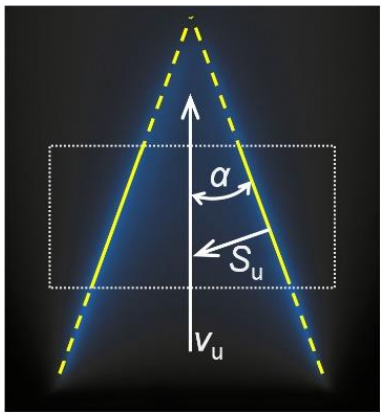

Figure 6. Relation between the laminar burning velocity (S_u), the cone angle (α), and the gas flow velocity (v_u) of a laminar premixed conical flame.

The uncertainties of the measured laminar burning velocities are based on the possible maximum error and calculated to be within a range of 2 cm/s and 7 cm/s, corresponding to relative errors between 3% and 8%, with values higher than 10% for fuel-rich or fuel-lean mixtures, especially at higher pressures. These uncertainties result primarily from the determination of the cone angle reflecting the difficulties during flame stabilization. Further effects on the accuracy of the measurement arise from pressure and temperature variations as well as from the accuracy of the mass flow controllers. For more information, the reader is also referred to our previous studies [16–18].

2.3. Modeling of Laminar Flame Speeds

The calculations of the laminar flame speeds of the diesel surrogate, OME_4, and the mixture diesel surrogate and 30% (*w*/*w*) OME_4 were done using an in-house reaction

mechanism [11]. A complete description of the oxidation of the diesel surrogate and OME_4 mixtures requires a mechanism that includes n-paraffins, iso-paraffins, and aromatics, as well as small alcohols and oxymethylene ethers. Not many literature mechanisms cover such a wide spectrum of molecular structures.

This reaction mechanism has been developed to cover a spectrum of several different fuels, ranging from road transportation to aviation, and comprises 70 validated hydrocarbon components of varying molecular structure as well as oxygenated fuel components. It includes reactions for the detailed description of most n-paraffins in the range of C_1–C_{16}, four iso-paraffins with a varying degree of branching, cyclo-paraffins such as single-ring cyclohexane, n-propylcyclohexane, bicyclic decalin, and cyclo-aromatics, such as indane, tetralin, and many (1-ring and multi-ring) aromatics. All these hydrocarbons are validated extensively against experiments from literature and from in-house data, covering measurements of species profiles, ignition delay times, and burning velocities. A detailed description of the reaction mechanism can be found elsewhere [11].

3. Results and Discussion

3.1. Results of the Sooting Propensity

Figure 7 shows the results from the determination of the sooting propensity. The experimental data are given in Table S1 of the Supplementary Material. As expected because of the non-existence of any C-C bonds within OME_n, the soot threshold of the diesel surrogate/OME_n mixtures is shifted to higher φ values with an increased OME_n content. A higher soot threshold correlates with a lower sooting propensity. Thus, in the present work, the amount of the OME_n addition to the diesel surrogate was clearly shown to have a significant influence on the sooting behavior.

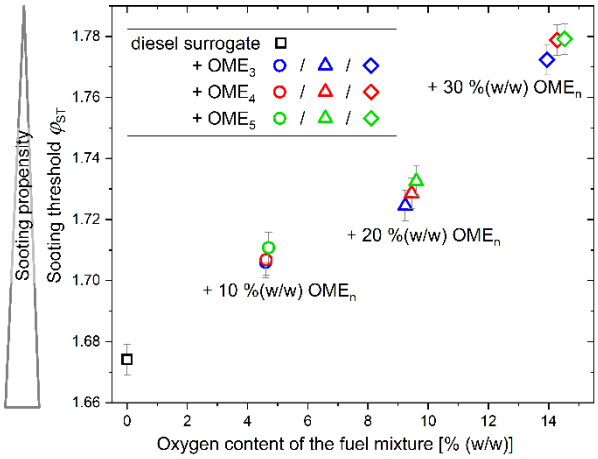

Figure 7. Results of the determined sooting propensities using the soot threshold (φ_{ST}) as indicator.

No evident dependence of the number of H_2CO groups in the specific OME_n molecule considered on the sooting propensity was experimentally observed. Figure 7 clearly reveals that the admixture, of either OME_3, OME_4, or OME_5, each lead to an increase of the sooting threshold and, therefore, to a reduction of the sooting propensity. However, the differences between the different OME_n are more or less in between the experimental uncertainty range of about ±0.005, determined by repeated measurements. Hence, it is inferred that an influence of the length of OME_n on the sooting propensity is not visible in the presence of a comparatively high sooting diesel surrogate.

The results shown here are in accordance with the basic knowledge regarding the sooting behavior of OME_n as well as in other studies, as from Omari et al. [5], Palazzo et al. [10], and Gaiser et al. [21,22]. Palazzo et al. [10] have measured the sooting propensity of a diesel fuel in a laminar diffusion flame using OME_2 and $OME_{3\text{-}5}$ as additives in concentrations of 1%, 3%, and 9% (each per volume). Even with an OME_n concentration of

1%, they have observed a distinct reduction of the sooting propensity with a slightly stronger effect of OME_{3-5}. Likewise, Omari et al. [5] and Gaiser et al. [21,22] found the reduction of soot formation independent of the OME_n chain length: Among others, Omari et al. [5] have studied the emissions of different OME_n and diesel blends in a single cylinder engine. Their results show reduced particulate matter emissions of the different blends compared to a pure diesel fuel. Gaiser et al. [21,22] have obtained species profiles in different low-pressure premixed OME_n flames. They found that the formation of C_2- and C_3-hydrocarbons during the combustion process—even at fuel-rich conditions—is very low and similar for OME_3, OME_4, and OME_5. As a result, no major soot precursors were detected, which explains the strong soot reduction potential, as found by Omari et al. [5] and Palazzo et al. [10] and shown in the present work [12] as well.

3.2. Results of the Laminar Burning Velocity

The results of the measured laminar burning velocities are displayed in Figure 8a, the corresponding data are provided in Tables S2–S10 in the Supplementary Material. At 1 bar, the maximum of the diesel surrogate located at φ = 1.1 yields about 83 cm/s (±2 cm/s). In contrast, OME_4 shows a distinct higher burning velocity with a maximum of 108 cm/s (±5 cm/s) being shifted to a higher φ value (φ = 1.2). Despite the specific percentage of OME_4 in the diesel surrogate mixture amounts, to up to 30% *(w/w)*, the LBV values are solely increased by about 4 cm/s to 87 cm/s (±2 cm/s) at φ = 1.1 the location of the peak value. As visible from Figure 8, similar findings were obtained for the measurements at 3 and 6 bar, with lower LBV values according to the higher set pressures.

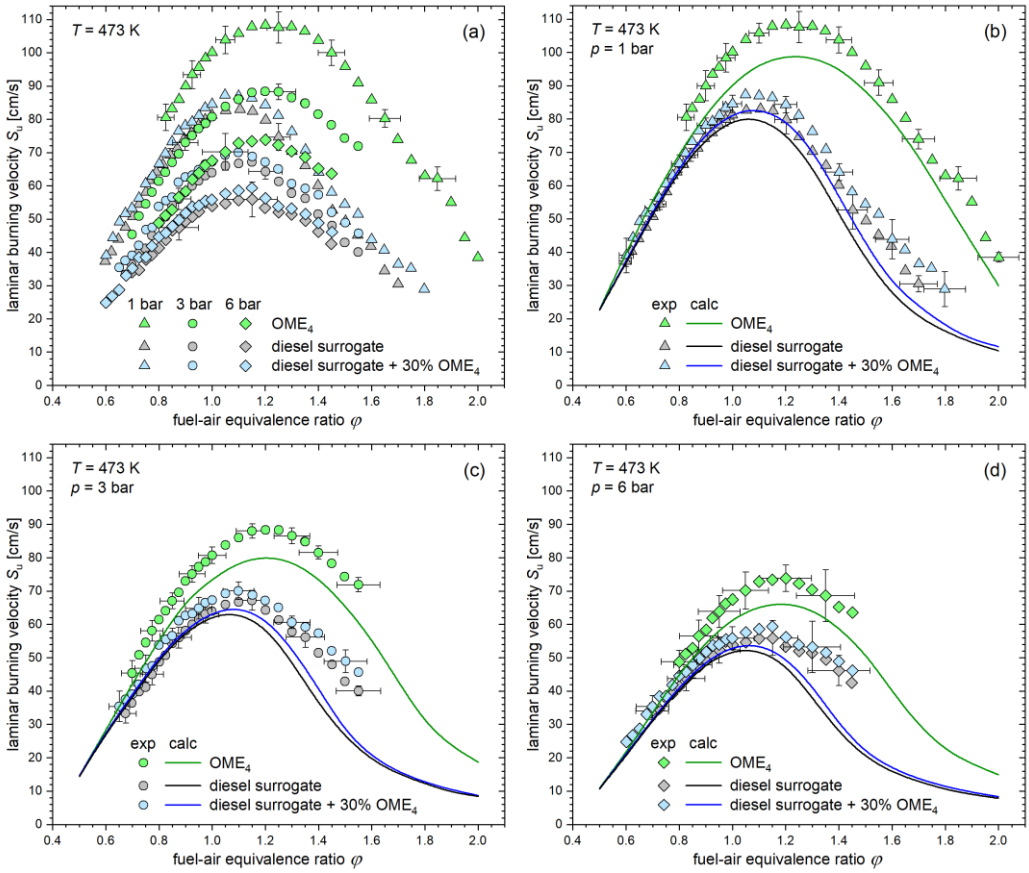

Figure 8. Results of the measured laminar burning velocities at T = 473 K of the diesel surrogate, neat OME_4, and diesel surrogate and 30% *(w/w)* OME_4 (**a**) and comparison between the experimental data and the calculated laminar flame speeds for 1 bar (**b**), 3 bar (**c**), and 6 bar (**d**).

To the best of our knowledge, experimental LBV data of OME_4 are presented for the first time; thus, allowing only for a comparison to literature data with other OME_n. In general, measurements of higher OME_n ($n \geq 2$) have been published by Sun et al. [7], Eckart et al. [8], and Ngugi et al. [9]. Sun et al. [7] have measured the LBV of OME_3 at 408 K and 1 atm with the peak value found at φ = 1.2 as well. The same findings were observed within the different studies of OME_2 from Eckart et al. [8] and Ngugi et al. [9], who have presented LBV values at various temperatures and pressures ranging, in total, from 383 K to 473 K and from 1 bar to 6 bar.

Figure 8b–d show the comparison between the measured LBV values and the calculated laminar flame speeds. For fuel-lean mixtures, the experimental data are reproduced reasonably by the mechanism; at $\varphi \geq 1.0$ the measured values are underpredicted by about 4 cm/s and up to 10 cm/s. These differences correspond to relative deviations between 3% and 10% for measurements at 1 bar as well as for stoichiometric and slightly fuel-rich mixtures at elevated pressures. At p = 3 bar and p = 6 bar, the deviations are higher for φ values >1.3, reflecting the more difficult flame stabilization within the experiments. However, nearly the same differences between the values of the laminar flame speed of pure OME_4, the diesel surrogate, and the diesel surrogate and OME_4 mixture were obtained from the modeling work. Hence, from the experimental as well as from the modeling work, it is concluded that the admixture of OME_4 to a diesel fuel (surrogate), even in significant amounts of 30% *(w/w)* as shown here, leads only to a small increase of the LBV values.

These findings are supported by another work from Ngugi et al. [23], where OME_1 is added with 30% *(w/w)* to PRF90 (primary reference fuel 90). Analog to this work, the LBV values of neat OME_1, PRF90, and the mixture PRF90 and 30% *(w/w)* OME_1 were investigated in an experimental and modeling study at the same conditions (T = 473 K, p = 1 bar / 3 bar / 6 bar). The obtained results in the OME_1-PRF90 study correspond to this work regarding the founded differences between OME_n, the surrogate/reference fuel, and the mixture with 30% OME_n. Therefore, it can be concluded that the decomposition and oxidation of hydrocarbons have a stronger influence on the reaction rate of OME_n-fuel blends than of OME_n. This is caused by the lower reactivity of hydrocarbons compared to OME_n, leading to lower LBV values.

4. Conclusions

Within the present study, the effect of the admixture in different amounts of OME_n to a widely used diesel fuel surrogate consisting of 50% n-dodecane, 30% farnesane (2,6,10-trimethyldodecane), and 20% 1-methylnaphthalene (mole percentages) was investigated. The foci were set on the sooting propensity and on the laminar burning velocity (LBV). The latter is a measure for the heat release as well as for the reactivity of any fuel and belongs to the global combustion properties. Thus, these data are needed and used to develop and optimize kinetic reaction mechanisms as well for the design of burner and burner chambers.

The present study of the sooting behavior of diesel surrogate and OME_n mixtures reveals that the admixture of OME_n (n = 3, 4, 5) to the diesel surrogate leads to a significant reduction of the sooting propensity. Regarding the length of the specific OME_n molecule, the measurements yield only a small effect that is almost negligible compared to the amount of OME_n in the fuel blend.

Regarding the laminar burning velocity (LBV) values, neat OME_4, the neat diesel surrogate, and a blend of the diesel surrogate with 30% OME_4 were investigated. To the best of our knowledge, LBV measurements of OME_4 and of a diesel and OME_4 mixture are reported for the first time. The burning velocity of OME_4 was found to be distinctly higher than the one of the diesel surrogate at all investigated pressures (p = 1 bar, 3 bar, and 6 bar). The admixture of 30% *(w/w)* OME_4 to the diesel surrogate leads to increased LBV values; however, much less than might be foreseen when looking at the respective values of the neat fuels.

Finally, the experimentally determined laminar burning velocities were compared with calculated laminar flame speeds using a recently developed in-house reaction mechanism. The modeling results match the experimental ones at fuel-lean conditions but underpredict the values determined of the stoichiometric and fuel-rich mixtures by up to 10 cm/s. Furthermore, the measured degree of differences between LBV values of pure OME_4, the diesel surrogate, and their blend is nearly identical to the one obtained with the modeling results. In summary, the reaction model is able to predict the measured LBV of the considered diesel surrogate, OME_4, and their blend, as well.

The results from the present work extend the data available in literature and help to understand the combustion characteristics of OME_n, especially of OME_4 and its mixture with a diesel surrogate. Both types of experiments were performed at the same conditions as well as with the same fuel mixture preparation and by using a similar burner configuration. Due to this, the findings of the present work demonstrate that OME_n show a reduction in soot particles when they are used as blending components to diesel fuels, without having any significant effect on the specific laminar burning velocity data. Therefore, reactivity and heat release of the fuel are similar. Future studies should focus on further major combustion properties, such as ignition delay times, to investigate the influence of OME_n on the ignition characteristics, as well as on the potential to an increased content of OME_n in diesel blends with the ultimate aim of achieving an even stronger reduction of soot emissions.

Supplementary Materials: The following are available online at www.mdpi.com/article/10.3390/en14237848/s1, Table S1: Results of the measured soot thresholds and Tables S2–S10: Experimental laminar burning velocities of OME_4/of the blend diesel surrogate and 30% *(w/w)* OME_4/of the diesel surrogate at a preheat temperature T = 473 K and p = 1 bar/p = 3 bar/p = 6 bar.

Author Contributions: Conceptualization, S.R. and M.B.-U.; methodology, S.R. and C.N.; modeling, T.K.; writing—original draft preparation, S.R. writing—review and editing, M.B.-U., T.K., C.N., and M.K.; supervision, C.N.; project administration, C.N. All authors have read and agreed to the published version of the manuscript.

Funding: This research received no external funding.

Data Availability Statement: All experimental data are available within the Supplementary Materials.

Acknowledgments: The authors thank Eleanor Adobeley Yankey (Kwame Nkrumah University of Science and Technology, Kumasi, Ghana) for her support measuring the sooting propensity.

Conflicts of Interest: The authors declare no conflict of interest.

References

1. Shamun, S.; Belgiorno, G.; di Blasio, G. Engine Parameters Assessment for Alcohols Fuels Application in Compression Ignition Engines. In *Alternative Fuels and Their Utilization Strategies in Internal Combustion Engines. Energy, Environment, and Sustainability*; Singh, A., Sharma, Y., Mustafi, N., Agarwal, A., Eds.; Springer: Singapore, 2020; pp. 125–139. https://doi.org/10.1007/978-981-15-0418-1_8.
2. Dreizler, A.; Pitsch, H.; Scherer, V.; Schulz, C.; Janicka, J. The role of combustion science and technology in low and zero impact energy transformation processes. *App. Energy Combust. Sci.* **2021**, *7*, 100040. https://doi.org/10.1016/j.jaecs.2021.100040.
3. Schemme, S.; Samsun, R.C.; Peters, R.; Stolten, D. Power-to-fuel as a key to sustainable transport systems—An analysis of diesel fuels produced from CO_2 and renewable electricity. *Fuel* **2017**, *205*, 198–221. https://doi.org/10.1016/j.fuel.2017.05.061.
4. *EN 590: Automotive Fuels-Diesel-Requirements and Test Methods*; German version EN 590:2013+A1:2017, Version DIN EN 590:2017-10, released October 2017. Available online: https://standards.iteh.ai/catalog/standards/cen/95e13683-15f8-4fa8-8009-2bb3867ca2b8/en-590-2013a1-2017 (accessed on 28 September 2021).
5. Omari, A.; Heuser, B.; Pischinger, S.; Rüdinger, C. Potential of long-chain oxymethylene ether and oxymethylene ether-diesel blends for ultra-low emission engines. *Appl. Energy* **2019**, *239*, 1242–1249. https://doi.org/10.1016/j.apenergy.2019.02.035.
6. Pélerin, D.; Gaukel, K.; Härtl, M.; Jacob, E.; Wachtmeister, G. Potentials to simplify the engine system using the alternative diesel fuels oxymethylene ether OME_1 and OME_{3-6} on a heavy-duty engine. *Fuel* **2020**, *259*, 116231. https://doi.org/10.1016/j.fuel.2019.116231.

7. Sun, W.; Wang, G.; Li, S.; Zhang, R.; Yang, B.; Yang, J.; Li, Y.; Westbrook, C.K.; Law, C.K. Speciation and the laminar burning velocities of poly(oxymethylene) dimethyl ether 3 (POMDME3) flames: An experimental and modeling study. *Proc. Combust. Inst.* **2017**, *36*, 1269–1278. https://doi.org/10.1016/j.proci.2016.05.058.
8. Eckart, S.; Cai, L.; Fritsche, C.; vom Lehn, F.; Pitsch, H.; Krause, H. Laminar burning velocities, CO and NOx emissions of premixed polyoxymethylene dimethyl ether flames, *Fuel* **2021**, *293*, 120321. https://doi.org/10.1016/j.fuel.2021.120321.
9. Ngugi, J.M.; Richter, S.; Braun-Unkhoff, M.; Naumann, C.; Köhler, M.; Riedel, U. A Study on Fundamental Combustion Properties of Oxymethylene Ether-2. *J. Eng. Gas Turbines Power* **2022**, *144*, 011014. https://doi.org/10.1115/1.4052097.
10. Palazzo, N.; Zigan, L.; Huber, F.J.T.; Will, S. Impact of Oxygenated Additives on Soot Propensity during Diesel Combustion, *Energies* **2021**, *14*, 147. https://doi.org/10.3390/en14010147.
11. Kathrotia, T.; Oßwald, P.; Naumann, C.; Richter, S.; Köhler, M. Combustion kinetics of alternative jet fuels, Part-II: Reaction model for fuel surrogate. *Fuel* **2021**, *302*, 120736. https://doi.org/10.1016/j.fuel.2021.120736.
12. Richter, S.; Kathrotia, T.; Braun-Unkhoff, M.; Naumann, C.; Köhler, M. Study on the influence of oxymethylene ethers (OME_n) blending a diesel surrogate. In Proceedings of the 10th European Combustion Meeting (ECM), Online, 14–15 April 2021.
13. Richter, S.; Kathrotia, T.; Naumann, C.; Scheuermann, S.; Riedel, U. Measurement of the sooting propensity of aviation fuel mixtures. In Proceedings of the 9th European Combustion Meeting, Lisboa, Portugal, 15–17 April, 2019; Paper Number S1_R1_74.
14. Richter, S.; Kathrotia, T.; Naumann, C.; Scheuermann, S.; Riedel, U. Investigation of the sooting propensity of aviation fuel mixtures. *CEAS Aeronaut. J.* **2021**, *12*, 115–123. https://doi.org/10.1007/s13272-020-00482-7.
15. Institute for Chemical Processes Engineering (ICVT), University Stuttgart, Stuttgart, Germany: Low-Pulsating Total Evaporation—The Solution for Precise Vapor Dosage. Available online: https://www.icvt.uni-stuttgart.de/verdampfer (accessed on 15 September 2021).
16. Kick, T.; Herbst, J.; Kathrotia, T.; Marquetand, J.; Braun-Unkhoff, M.; Naumann, C.; Riedel, U. An experimental and modeling study of burning velocities of possible future synthetic jet fuels. *Energy* **2012**, *43*, 111–123. https://doi.org/10.1016/j.energy.2012.01.035.
17. Richter, S.; Kathrotia, T.; Naumann, C.; Kick, T.; Slavinskaya, N.; Braun-Unkhoff, M.; Riedel, U. Experimental and modeling study of farnesane. *Fuel* **2018**, *215*, 22–29. https://doi.org/10.1016/j.fuel.2017.10.117.
18. Methling, T.; Richter, S.; Kathrotia, T.; Braun-Unkhoff, M.; Naumann, C.; Riedel, U. An investigation of Combustion Properties of Butanol and Its Potential for Power Generation. *J. Eng. Gas Turbines Power* **2018**, *140*, 091505. https://doi.org/10.1115/1.4039731.
19. Andrews, G.; Bradley, D. Determination of burning velocities: A critical review. *Combust. Flame* **1972**, *18*, 133–153. https://doi.org/10.1016/S0010-2180(72)80234-7.
20. Eberius, H.; Kick, T. Stabilization of premixed, conical methane flames at high pressure. *Ber. Bunsenges. Phys. Chem.* **1992**, *96*, 1416–1419. https://doi.org/10.1002/bbpc.19920961013.
21. Gaiser, N.; Bierkandt, T.; Zhang, H.; Schmitt, S.; Oßwald, P.; Zinsmeister, J.; Hemberger, P.; Shaqiri, S.; Kasper, T.; Kohse-Höinghaus, K.; et al. Systematic study on laminar low-pressure oxymethylene ether (OME_{0-4}) flames using molecular beam mass spectrometry and synchrotron photoionization. In Proceedings of the 30. Deutscher Flammentag, Hannover-Garbsen, Germany, 28–29 September 2021.
22. Gaiser, N.; Bierkandt, T.; Oßwald, P.; Shaqiri, S.; Zinsmeister, J.; Kathrotia, T.; Hemberger, P.; Köhler, M.; Kasper, T.; Aigner, M. Oxidation of oxymethylene ether (OME_{0-5}): An experimental systematic study by mass spectrometry and photoelectron photoion coincidence spectroscopy. *Fuel* **2021**, accepted.
23. Ngugi, J.M.; Richter, S.; Braun-Unkhoff, M.; Naumann, C.; Riedel, U. A study on fundamental combustion properties of oxymethylene ether-1/primary reference fuel blend: Experiments and modeling approach. *Combust. Flame*, Under Review.